# Hollow Cathodes Study at Alta-Centrospazio

**IEPC-2005-277**
*Presented at the 29th International Electric Propulsion Conference, Princeton University, October 31 - November 4, 2005*

Rossetti, P.*, Signori, M.°
*Alta SpA-Centrospazio, Pisa, I-56121, Italy*

Andrenucci, M.♣, Paganucci, F♦
*University of Pisa, Pisa, I-56100, Italy.*

**For several years a research activity has been carried out at Alta-Centrospazio on hollow cathode models for both single- and multiple-channel configurations. A review of the single-channel model is presented in the first part of the paper. In the light of a certain discrepancy between numerical and experimental results, the adopted ionisation mechanism is discussed as the most probable responsible for this fact and a most suitable process is presented in order to improve model prediction capability. In the second part the paper deals with the multiple-channel hollow cathode model developed by Alta-Centrospazio more recently for application to high-current hollow cathodes design for MPD thrusters.**

## Nomenclature

Constants:

$A_r$ = Richardson constant, $1.2 \cdot 10^6$ $A/(m^2K^2)$
$e$ = Elementary charge, $1.602 \cdot 10^{-19}$ $C$
$k_b$ = Boltzmann constant, $1.38 \cdot 10^{-23}$ $J/K$
$m_e$ = Electron mass, $9.11\ 10^{-31}$ $kg$
$a.m.u.$ = Atomic mass unit, $1.66 \cdot 10^{-27}$ $kg$
$\varepsilon_o$ = Vacuum dielectric constant, $8.85 \cdot 10^{-12}$ $F/m$
$\sigma$ = Stefan-Boltzmann constant, $5.67 \cdot 10^{-8}$ $W/(m^2K^4)$

For Single-channel Hollow Cathode Model:

$C_p$ = Specific heat
$E$ = Electric field in the cathode sheath
$I$ = Current
$j_{re}$ = Thermionic current density
$j_{ri}$ = Ionic current density
$j_x$ = Current density in the plasma column
$j_{x\_cat}$ = Current density in the cathode body
$l$ = Cathode length
$m\_dot$ = Mass flow rate

* Project Manager, Alta SpA-Centrospazio, p.rossetti@alta-space.com.
° Project Engineer, Alta SpA-Centrospazio ,m.signori@alta-space.com.
♣ Full Professor, Department of Aerospace Engineering, m.andrenucci@alta-space.com.
♦ Associate Professor, Department of Aerospace Engineering, f.paganucci@alta-space.com.

$M$ = Atomic or ion mass
$n_e$ = Electron or ion density
$n_o$ = Neutral density
$Q_s$ = Cross-section for the generic collision experienced by the electron
$Q_{ion}$ = Ionization collision cross-section
$r$ = Cathode radius
$t$ = Cathode wall thickness
$T_W$ = Cathode wall temperature
$T_e$ = Electronic temperature
$\bar{v}$ = Mean flow velocity
$V$ = Plasma potential
$V_i$ = Atom ionization potential
$X_i$ = Ionization degree

$\varepsilon$ = Surface emissivity
$\varphi$ = Surface work function
$\gamma$ = Specific heats ratio
$\lambda_t$ = Cathode thermal conductivity
$\mu$ = Viscosity coefficient
$\sigma_{el}$ = Plasma electrical conductivity
$\rho$ = Cathode electrical resistivity

For Multiple-channel Hollow Cathode Model:

$A$ = Shape factor
$D_{eq}$ = Equivalent diameter
$I$ = Discharge current
$k_t$ = Thermal conductivity
$\dot{m}$ = Mass flow rate
$Q$ = Mass flow rate
$\dot{Q}_{Joule}$ = Power density due to Joule heating
$\dot{Q}_{jre}$ = Power density due to electron emission
$\dot{Q}_{jri}$ = Power density due to ion bombardment
$\dot{Q}_{rad}$ = Power density due to radiation
$r_0$ = Radius of the internal tube
$S$ = Cross section area
$T$ = Temperature

## I. Introduction

The development of long-life cathodes represents a crucial issue for high power electric propulsion technology. Cathode lifetime strongly depends on cathode operating temperature and current distribution over its surface.

In a Single-channel Hollow (ScH) cathode operating in the so-called *normal* (or *spot*) regime, an internal plasma column (IPC) forms which drives the discharge current from the external anode-cathode region to the internal cathode wall, called active zone (AZ). In this condition a larger electrode surface is interested by the discharge current with respect to a rod cathode, allowing lower temperature values[1]; moreover since propellant ionization taking place in the cathode cavity is more efficient, less electron emission is required and by consequence surface temperature is further reduced. Other beneficial effects have been shown by HC-based devices, as lower anode-cathode voltage drop for the same current, smoothing of current and voltage fluctuations and reduction of plasma contamination, which is a direct consequence of cathode erosion attenuation.

As a matter of fact the most performing cathodes in the electric propulsion field have a single-channel configuration as in EB ion and Hall-effect engines. Anyway for high power application at current levels above 20 A, cathode technology seems still no enough mature in order to provide with reliable components.

For applications to MPD thrusters operating at power level from 10 kWe up to 1 MWe, Multiple-channel Hollow (McH) cathodes are more appropriate as shown by Li-fed MPD thrusters advanced laboratory models[2, 3].

As a matter of fact McH cathodes have been conceived for operation at high current levels and/or relatively low mass flow rates[4]. Increasing the operation current of a ScH cathode, channel diameter should be increased for lifetime concern and by consequence also the mass flow rate in order to avoid a longer IPC (or even the impossibility for the cathode to operate in the normal regime) with a strong penalty on the efficiency side. In general this mass flow rate augmentation could not be compatible with the pumping system capacity and in the special case of MPD thruster application with thruster performance in terms of specific impulse or thrust efficiency.

In practice the McH cathode consists of a bundle of little tubes or rods, housed in a main tube (*macaroni packet*). Main features of this kind of devices with respect to the ScH cathode are their capability of sustaining a higher current at the same external diameter and a lower *I-V* characteristics; this last circumstance is due to the reduction of the IPC length and then of the cathode voltage drop. Moreover at the same operating conditions in terms of mass flow rate and discharge current, the wall temperature profile is lower for a McH than for a ScH cathode, with important implications on the electrode lifetime. Finally another interesting feature of McH cathodes is their capability to be ignited and to sustain lower current levels than ScH cathodes, grace to the partial activation of the cathode with the number of ignited channels reducing with current decreasing.

Considering the great importance of HCs in electric propulsion, for a few years Alta-Centrospazio has carried out theoretical and numerical studies on this type of devices. In previous papers[5, 6] both single-channel and multiple-channel cathode models are described and discussed. More recent developments on this topic are presented in the following.

## II. Review of the Single-channel Hollow Cathode Model

Since 2000, Centrospazio has developed a one-dimension, stationary HC model, able to predict plasma parameters (electron/ion temperature and density and plasma potential), cathode temperature and electron/ion current densities distributions along the channel axis as a function of cathode geometry and material properties, gas characteristics and mass flow rate and plasma potential drop at the cathode outlet.

An accurate description of the mathematical model can be found in Ref. 5. Hereafter the system of six differential equations and of six algebraic equations describing the physics of hollow cathode phenomenon is reported:

1- The thermal balance of the cathode body, comprising power inputs due to Joule effect and to ion bombardment, and power outputs deriving from thermionic emission, surface radiation and heat conduction to the incoming gas

$$-\frac{d}{dx}\left(\lambda_t \cdot \frac{dT_w}{dx}\right) = \rho \cdot j_{x\_cat}^2 + \left(\frac{1}{t}\right)\cdot\left(j_{ri}\cdot\left(V + V_i - \varphi_{eff}\right)\right) - \left(\frac{1}{t}\right)\cdot\left(j_{re}\cdot\eta_{ion}\cdot\varphi_{eff}\right) +$$

$$-\left(\frac{1}{t}\right)\cdot\left(\left(1+f_v\right)\cdot\sigma\cdot\varepsilon\cdot T_w^4\right) - \left(\frac{1}{t}\right)\cdot\frac{C_p\cdot\dot{m}\cdot\frac{dT_w}{dx}}{2\cdot\pi\cdot r} \qquad (1)$$

2- The electrons temperature equation (ions and neutrals temperatures are assumed equals to $T_W$)

$$\frac{d}{dx}\left(j_x\cdot T_e\cdot\frac{3.2\cdot k_b}{e}\right) = j_x\frac{dV}{dx} + \left(\frac{2}{r}\right)\cdot\eta_{ion}\eta_{out}\cdot j_{re}\left(V - V_i\right) \qquad (2)$$

3- Momentum equation for the gas flow from the Poiseuille theory, corrected for the sliding effect at the wall

$$\frac{dP}{dx} = -\xi_{ck}\cdot\frac{\mu\cdot 8\cdot\bar{v}}{r^2} \qquad (3)$$

4- Balance equation for plasma current and cathode body current

$$\frac{dj_x}{dx} = \frac{2}{r} \cdot \left( j_{re} \cdot \eta_{ion} + j_{ri} \right) \tag{4}$$

$$\frac{dj_{x\_cat}}{dx} = -\frac{1}{t} \cdot \left( j_{re} \cdot \eta_{ion} + j_{ri} \right) \tag{5}$$

5- The Ohm law for potential field calculation

$$j_x = \sigma_{el} \cdot \left( \frac{dV}{dx} - \frac{1}{n_e \cdot e} \cdot \frac{d\left(T_e \cdot k_b \cdot n_e\right)}{dx} \right) \tag{6}$$

The algebraic equations are:

$$P = \left(n_o + n_e\right) \cdot k_b \cdot T_w \cdot \left( 1 + \frac{T_e}{T_w} X_i \right) \tag{7}$$

$$X_i = \frac{n_e}{n_o + n_e} \tag{8}$$

$$j_{ri} = j_{re} \cdot \eta_{ion} \cdot \eta_{out} \tag{9}$$

$$j_{ri} = \alpha_2 \cdot n_e \cdot \sqrt{\frac{k_b \cdot T_w}{M}} \tag{10}$$

$$j_{re} = A_R \cdot T_w^2 \cdot e^{-\left(\frac{e \cdot \varphi_{eff}}{k_b \cdot T_w}\right)} \tag{11}$$

$$\varphi_{eff} = \varphi - \sqrt{\frac{e \cdot E}{4 \cdot \pi \cdot \varepsilon_o}} \tag{12}$$

**A. Model improvements**

One of the major point of discussion about the ScHC model is the choice of the ionisation mechanism inside the channel. In the present model we adopted the single-step ionisation mechanism proposed in the early studies on HC phenomenon by Delcroix et al.: each ion forms by a single collision between a neutral and a primary electron, i.e. emitted by the cathode surface, that has acquired enough energy crossing the potential field in the cathode sheath.

Considering a single-step ionisation mechanism, primary electrons entering the main plasma column must have an energy at least equals to the first ionisation energy of the neutral atom. This means that electrons emitted by surface zones along the cathode axis where plasma potential is lower than $V_i$ can not contribute to atoms ionisation; as a consequence those zones would cool down since not ion bombardment takes place at the corresponding abscissas along the cathode and at the end electrons emission would stop. In practice the condition $V = V_i$ represents the boundary between the active and non-active zones inside the channel.

As a matter of fact from the point of view of the solving algorithm, the plasma potential differential equation (6) is integrated upstream from the cathode outlet and the plasma potential is put equal to zero after passing the abscissa where $V = V_i$.

At the end Eq. (9) derives from considering that in the active zone each emitted electrons experiences an ionisation collision with a neutral, except for those electrons whose mean free path (*m.f.p.*) allows them to reach the opposite wall or to escape from cathode outlet. These two electrons losses are accounted by the coefficient $\eta_{ion}$ and $\eta_{out}$ respectively.

Both coefficients depend on geometrical characteristics and on primary electrons *m.f.p.* between two consecutive ionization collisions, evaluated as:

$$m.f.p. = \left( \frac{\sum_s n_s Q_s}{n_o Q_{ion}} \right)^{0.5} \frac{1}{\sum_s n_s Q_s}$$

where the sum is extended to all types of collision undergone by the electrons. Finally, it results:

$\eta_{ion} = 1\text{-}\exp(2r/m.f.p.)$

$\eta_{out} = 0.5(1+(l\text{-}x)/m.f.p.)$ if $m.f.p.>2(l\text{-}x)$

$\eta_{out} = 1$ if $m.f.p.<2(l\text{-}x)$

Numerical results tend to underestimate the current obtainable by a set of operating conditions for a given cathode geometry or analogously to overestimate the plasma potential at the cathode outlet for a desired current value.

This fact pushes the authors to investigate more deeply the ionisation mechanism. At this purpose cross sections for primary electron-atom ionisation process and primary electron- plasma electron collision have been evaluated and compared, under typical plasma condition inside the channel and assuming a Maxwell distribution for electrons temperature in the main plasma.

As reported in Fig. 1, cross section for primary electron-plasma electron collision is some orders of magnitude higher than cross section for primary electron-atom ionisation. In the light of this result the ionisation mechanism considered in the frame of the present model has been changed: atom ionisation is still a single-step process but it takes place between neutrals and the maxwellian electrons population. Eq. (9) is then substituted by:

$$j_{ri} = eW_{ion} \cdot \frac{r}{2}$$

where the ionisation rate has the expression

$$W_{ion} = n_e n_o \alpha_{ion}$$

with the ionisation rate coefficient calculated as:

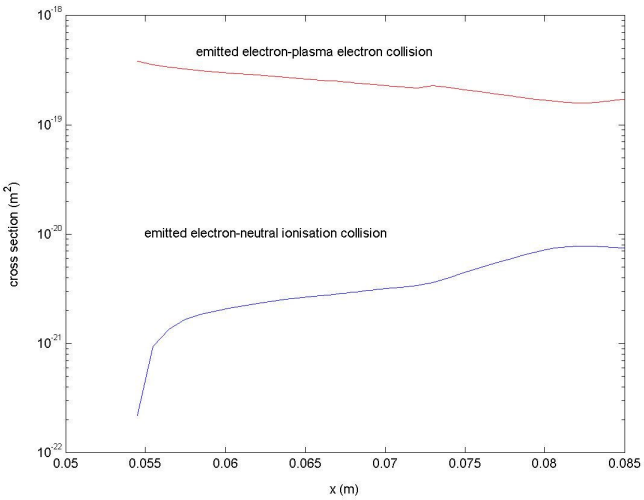


**Figure 1. Cross sections comparison for emitted electron-plasma electron collision and emitted electron-neutral ionisation inside hollow cathode**

$$\alpha_{ion}(T_e) = 4\pi\left(\frac{m_e}{2\pi kT_e}\right)^{\frac{3}{2}} \int_{\sqrt{\frac{2V_i}{m_e}}}^{\infty} g^3 \exp\left(\frac{m_e g^2}{2kT_e}\right) Q_{ion}(g)\,dg$$

In the above expression $Q_{ion}$ is the cross section for atom-electron ionisation impact.

This modification has also important consequence on the solving algorithm. The new set of equations allows for fixing the current as input parameter, instead of the plasma potential at the outlet; the potential differential equation can be integrated starting from the cathode inlet with $V= 0$ as boundary condition, since there is no more the need to establish the abscissa where $V= V_i$ in order to arbitrarily put equals to zero some quantities like $V$, $j_{re}$, $n_e$ for the upstream abscissas. With the new ionisation mechanism the ionisation rate is everywhere different from zero since electrons in the maxwellian distribution tail are capable of producing ions.

At the state of the art the new ionisation mechanism has already been integrated to the rest of HC model and the new solving algorithm is under development.

## III. Multiple-channel Hollow Cathode Model

While ScHC model improvement activity, a Multiple-channel HC model has been developed on the base of the ScHC model previously described.

The McHC model aims to allow for investigation of different configurations in which such a type of cathode can be conceived; Fig. 2 reports those configurations in a schematic way. McHC obtained by a bundle of tungsten sticks housed in a main tungsten tube is the most common configuration since it is the easiest to manufacture, but early studies by Delcroix considered other configurations like that obtained with a bundle of little tubes and as the most promising that formed by concentric tubes.

In our model already presented in a previous paper as well as some preliminary results, we considered first a McH cathode formed by seven equal cylindrical tubes regularly disposed in a main tube. The limited number of considered channels makes the analysis suitable for a low current discharge; for high current discharges typical of MPD thruster applications channels number in McHC are in the order of several tens. Unfortunately the complexity of the numerical model and the required solving time grow up exponentially for each added channel.

On the other end, as preliminary results have shown, the chosen geometry already allows to highlight some characteristic behavior of McH cathodes.

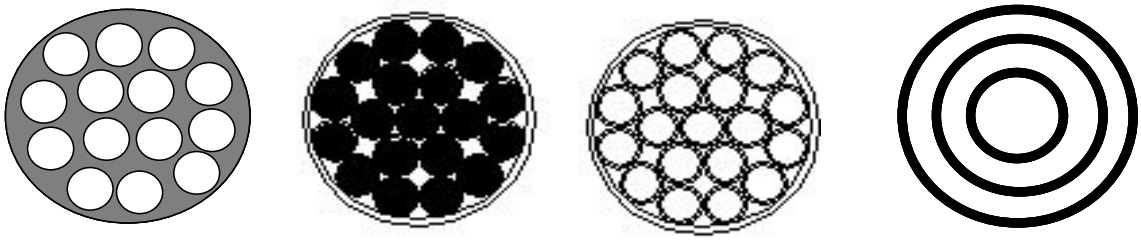

**Figure 2. Different McHC configurations**

About geometrical parameters, the model allows to vary diameter and thickness of the internal tubes, while the internal diameter of the main tube is calculated by consequence and its thickness is again a free input parameter.

Consideration on problem symmetry allows to study an angular sector of $\pi/3$, as highlighted in Fig.3. At each cathode cross section along the x-axis, the model considers one plasma node for each of the four channels (Tp1, Tp2, Tp3, Tp4 in Fig. 3) and a total of ten material nodes in order to account for temperature gradient along the circumference of each cylindrical channels.

For calculating plasma parameters and gas-dynamic quantities along the four plasma channels the same equations system of the ScH cathode model has been applied, but:

1- the ion/neutral temperature in each channel is calculated as average of the temperature values in the nodes of the corresponding channel wall,

2- the mass flow rate distribution among the four channels is calculated as:

$$\frac{\dot{m}(j_P+1)}{\dot{m}(j_P)} = \frac{S(j_P+1)\cdot\left[D_{eq}(j_P+1)\right]^2 \cdot A(j_P)}{S(j_P)\cdot\left[D_{eq}(j_P)\right]^2 \cdot A(j_P+1)}\left[\frac{T(j_P)}{T(j_P+1)}\right]^{3/2}$$

where $S$, $D_{eq}$, $A$ and $T$ refer to the generic $j_P$ channel.

Concerning the thermal balance of channels wall, with respect to the ScHC model, some terms have been added accounting for energy exchanges with plasma wetting the external channel surface and heat conductivity along the circumference due to the non-zero temperature gradient in that direction. At the end the thermal balance equation for a finite element of volume $V$ centered on the generic $j$-th, $k$-th material node (with $j$ and $k$ referring to nodes numbering along the angular coordinate $r_0\Psi$ and the channel axis $x$) is:

$$k_t(T_{j,k})\cdot\left[\left(\left(\frac{T_{j,k+1}-T_{j,k}}{dx_k}+\frac{T_{j,k-1}-T_{j,k}}{dx_{k-1}}\right)\cdot S_x+\left(\frac{T_{j+1,k}-2T_{j,k}+T_{j-1,k}}{r_0 d\psi}\right)\left(\frac{S_\psi(k-1)+S_\psi(k)}{2}\right)\right)\right]+$$
$$+\left[\dot{Q}_{Joule}(j,k)+\dot{Q}_{jri}(j,k)+\dot{Q}_{jre}(j,k)+\dot{Q}_{rad}(j,k)\right]\frac{V_{k-1}+V_k}{2}=0$$

where $S_x$ and $S_\Psi$ refer to the area of element surfaces perpendicular to $x$ and $\Psi$ respectively.

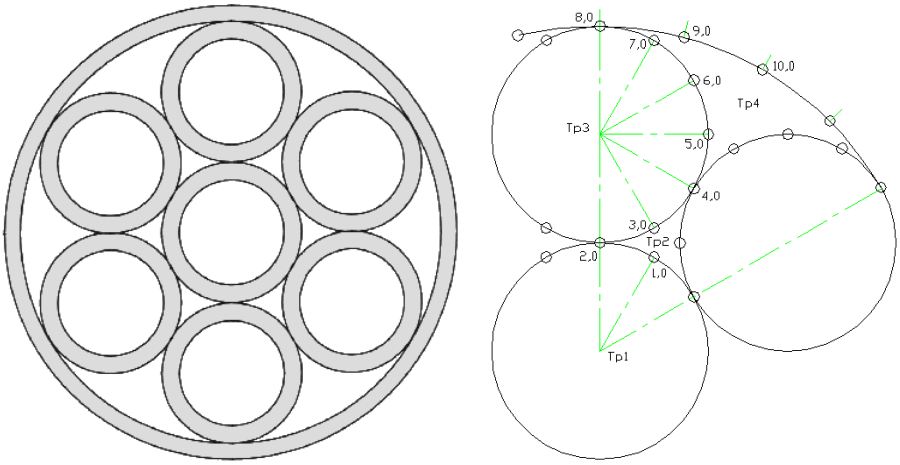


**Figure 3. Schematic of the McH cathode geometry (on the left, thickness walls not in scale) and nodes considered by the model (on the right).**

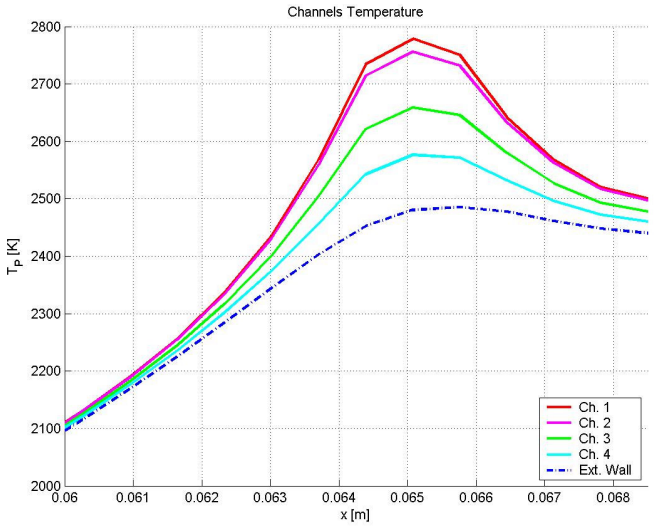


**Figure 4 Temperature profiles for the four plasma channels and the external wall**

Fig. 4 shows temperature profiles along the four plasma channels and the external cathode wall, for a McH cathode with main tube radius and length of 2.06 mm and 68.5 mm respectively, operating with argon at 1.2 mg/s and at a discharge current of 2.3 A. As expected and verified experimentally also in Li-fed MPD thrusters, since the main cooling mechanism for this type of cathode is surface radiation, temperature profile grows up going from the external tube to the inner channels. Moreover the position of the temperature peak shifts downstream going from the center of the cathode towards its external boundary; this is an effect of the different mass flow rate distribution among channels: cooler channels are interested by higher gas flows which tend to blow out the plasma column; macroscopically this effect is measured by the temperature peak displacement towards the cathode exit.

Fig. 5 allows for a comparison between ScHC and McHC in terms of cathode temperature at the same operating current and mass flow rate. Together with temperature profiles of the external tube and of the innermost plasma channel for the McHC, the temperature profile for a ScH cathode with the same external diameter and thickness of the McHC external tube has been reported. Temperature profile for the ScH cathode is much higher and steeper in the active zone; moreover the peak position is more internal than for the McH cathode. This last occurrence would imply the IPC is longer and then the total voltage drop is greater for the ScH (35 V) than for the McH cathode (22 V).

With minor modifications, without increasing the complexity of the solving algorithm, on the contrary in some cases simplifying the equations system, the McHC model can be modified for accounting for all other different configurations, as that deriving from considering a bundle of seven sticks, with plasma channels formed by spaces among sticks, or the complementary configuration obtainable from drilling seven channels in a full matrix.

As said before one of the most interesting McHC configuration is that formed by concentric tubes; As reported in Fig. 6 from Delcroix, this configuration can have further improvement with respect to ScHC in terms of lower operating temperature.
The current activity on McHC model aims to adapt it to the concentric-channels configuration

## IV. Conclusions

For some years Alta has carried out an intensive research activity aimed to the development of hollow cathode models, both for ScHC than for McHC as powerful tools for cathode design, especially for high power applications.

In this frame a quite sophisticated ScHC model has been developed first. The model gave satisfying results, but further improvements are within to be achieved, by considering a more realistic ionisation mechanism taking place inside the plasma column with respect to the simple one-step ionisation process between neutral and primary electron.

A preliminary McHC model has been developed more recently and it has been revisited in the present paper together with first encouraging results.

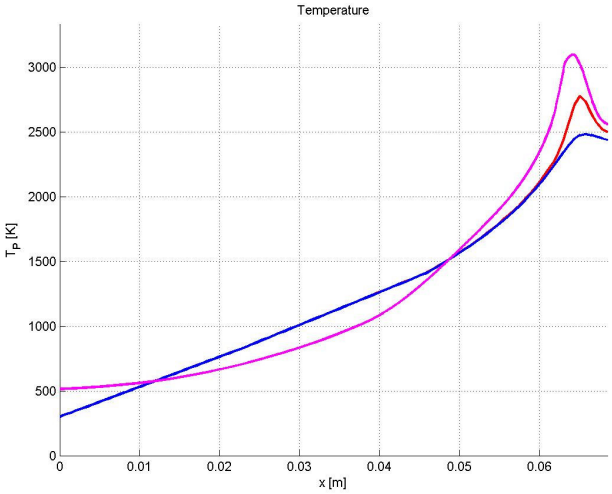


**Figure 5. Temperature profile for the ScH cathode (pink) and for the McH cathode (blue: main tube wall, red: innermost plasma channel) operating at the same conditions**

In the next future McHC model will be modified for analyzing different channels arrangements, in order to highlight advantages and drawbacks of different configurations. Although the model is suitable for low current applications (little channels number), results from different configurations comparison are probably extendable to larger cathodes and operating currents.

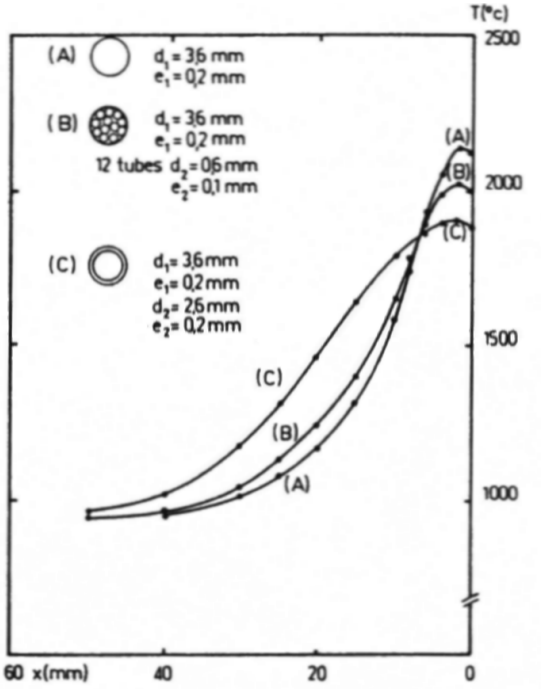


**Figure 6. From Ref. 4. Comparison among single channel, macaroni packet and concentric-channels cathodes**

## References


1 Delcroix, J., et al., "Hollow Cathode Arcs", *Adv. in Electronics and Electron Phys*., Vol. 35, 1974.

2 Choueiri, E., et al., "Lorentz Force Accelerator with an Open-ended Lithium Heat Pipe", AIAA-96-2737, *32nd Joint Propulsion Conference*, July 1996, Lake Buena Vista, FL

3 Tikhonov, V.B., Semenikhin S. A., Polk, J. E., and Brophy, J. R., "Performance of 130 kW MPD Thruster with an External Magnetic Field and Li as Propellant", IEPC-97-117, *25th International Electric Propulsion Conference*, Aug. 1997, Cleveland, OH.

4 Delcroix J. L., Minoo H., and Trindade A. R., *Rev. of Scient. Instr.*, Vol. 40, No. 12, Dec. 1969, pp. 1555-1562.

5 Rossetti, P., Paganucci, F., and Andrenucci, M., "A Hollow Cathode Model for Application to the Electric Propulsion", AIAA-2002-4239, *38th Joint Propulsion Conference*, July 7-10, 2002, Indianapolis, IN.

6 P. Rossetti, F. Paganucci, M. Andrenucci, M. Signori, "*Centrospazio Progress on MPDT Hollow Cathodes"* AIAA-2004-3429, 40th Joint Propulsion Conference, July 11-14, 2004, Fort Lauderdale, FL.